Synthesis, Characterization, and Properties of an Open-Framework Iron(III) Dicarboxylate: MIL-85 or $Fe^{III}_2O\{O_2C-CH_3\}_2\{O_2C-C_6H_4-CO_2\}\cdot 2CH_3OH$

Christian Serre,*,† Franck Millange,† Suzy Surblé,† Jean-Marc Grenèche,‡ and Gérard Férey†,§

Institut Lavoisier-Franklin, UFR 2483, Université de Versailles St-Quentin-en-Yvelines, 45 Avenue des Etats-Unis 78035 Versailles Cedex, France, and Laboratoire de Physique de L'Etat Condensé, UMR CNRS 6087, Université du Maine, 72085 Le Mans Cedex 9, France

Received March 19, 2004. Revised Manuscript Received April 20, 2004

A new three-dimensional iron(III) dicarboxylate, **MIL-85** or $Fe^{III}_2O\{O_2C-CH_3\}_2\{O_2C-C_6H_4-CO_2\}\cdot 2CH_3OH$, has been obtained under solvothermal conditions, and its structure was determined using X-ray powder diffraction data. Its chiral framework is built up from helical chains of iron(III) octahedra linked through terephthalate dianions. This creates a three-dimensional structure with an array of 1-D small-pore channels filled with free and bound methanol moieties. The thermal behavior has been investigated using TGA, and X-ray thermodiffractometry indicates that **MIL-85** is stable up to 275 °C with a fully reversible departure of solvent process. When the free and bound solvent molecules are removed, a nanoporous solid with a Langmuir surface area of 110 m^2/g is obtained. Mössbauer spectrometry confirms the presence of high-spin-state Fe^{3+} within the structure and a change in the iron environment upon solvent departure. Finally, one can conclude from magnetic data that **MIL-85** exhibits a frustrated magnetic behavior in the low-temperature range. Crystal data for **MIL-85**: hexagonal space group $P6_1$ (n*o*. 169) with $a = 11.045$ (1) Å, $c = 18.823$ (1) Å, and $Z = 6$.

Introduction

In the field of porous solids, the synthesis of hybrid inorganic−organic compounds is an interesting alternative method[1−5] to obtain large-pore solids with tunable properties such as magnetism,[6] hydrogen storage,[7,8] optical properties,[9] and catalysis.[10] This is due to the large number of possible associations between inorganic clusters, chains, or layers and various organic moieties such as carboxylates and phosphonates. The concept of reticular chemistry proposed by Yaghi and O'Keeffe[11] has rationalized the rules for the synthesis of these metal−organic frameworks: linkage of known inorganic moieties with the desired organic ligand. The difficult point, increased by the use of hydrothermal synthesis, concerns the design of the inorganic clusters and the corresponding mastered chemistry. For some of them, spectacular results were obtained with zinc metal organic frameworks (MOFs) that exhibit both a large and a modulable porosity.[5]

In the field of metalocarboxylates, hydrothermally synthesized three-dimensional porous or pillared solids have been reported with divalent cations such as zinc,[11,12] copper,[13] nickel,[14,15] iron,[16,17] and cobalt.[18,19] However, these approaches are not easily applicable to higher oxidation state elements, and porous three-dimensional hybrid solids based on tri- or tetravalent cations are still scarce. Recently, the study of a three-dimensional indium dicarboxylate was reported,[20] while our group also characterized several open-framework

* To whom correspondence should be addressed. E-mail: serre@chimie.uvsq.fr.
† Université de Versailles St-Quentin-en-Yvelines.
‡ Université du Maine.
§ Present affiliation: Institut Universitaire de France.

(1) Robl, C. *Mater. Res. Bull.* **1992**, *27*, 99.
(2) Clearfield, A. *Curr. Opin. Solid State Mater. Sci.* **1996**, *1*, 268.
(3) Feng, S.; Xu, R. *Acc. Chem. Res.* **2001**, *34*, 239.
(4) Férey, G. *Chem. Mater.* **2001**, *13*, 3084−3098.
(5) Eddaoudi, M.; Moler, D. B.; Li, H.; Chen, B.; Reineke, T.; O'Keefe, M.; Yaghi, O. M. *Acc. Chem. Res.* **2001**, *34*, 319.
(6) Férey, G. *Nat. Mater.* **2003**, *2*, 136−137.
(7) Rosi, N. L.; Eckert, J.; Eddaoudi, M.; Vodak, D. T.; Kim, J.; O'Keeffe, M.; Yaghi, O. M. *Science* **2003**, *300*, 1127−1129.
(8) Férey, G.; Latroche, M.; Serre, C.; Millange, F.; Loiseau, T.; Percheron-Guégan, A. *Chem. Commun.* **2003**, 2976.
(9) Serpaggi, F.; Férey, G.; Antic-Fidancev, E. *J. Solid State Chem.* **1999**, *148*, 347−352.
(10) Seo, J. S.; Whang, D.; Lee, H.; Jun, S. I.; Oh, J.; Jeon, Y. J.; Kim, K. *Nature* **2000**, *404*, 982.
(11) Yaghi, O. M.; O'Keeffe, M.; Ockwig, N. W.; Chae, H. K.; Eddaoudi, M.; Kim, J. *Nature* **2003**, *423*, 705.
(12) Erxleben, A. *Coord. Chem. Rev.* **2003**, *246*, 203−228.
(13) Chui, S. S.-Y.; Lo, S. M.-F.; Charmant, J. P.; Orpen, A. G.; Williams, I. D. *Science* **1999**, *283*, 1148.
(14) Forster, P. M.; Cheetham, A. K. *Angew. Chem., Int. Ed.* **2002**, *41*, 457.
(15) Guillou, N.; Livage, C.; Drillon, M.; Férey, G. *Angew. Chem. Int. Ed.* **2003**, *42*, 5314.
(16) Sudik, A. C.; Yaghi, O. M. *Abstr. Pap. Am. Chem. Soc.* **2002**, *223*, A40−A40.
(17) Sanselme, M.; Grenèche, J. M.; Riou-Cavellec, M.; Férey, G. *Chem. Commun.* **2002**, 2172−2173.
(18) Huang, Z.-L.; Drillon, M.; Masciocchi, N.; Sironi, A.; Zhao, J.-T.; Rabu, P.; Panissod, P. *Chem. Mater.* **2000**, *12*, 2805.
(19) Livage, C.; Guillou, N.; Marrot, J.; Férey, G. *Chem. Mater.*, **2001**, *13*, 4387.
(20) Gomez-Lor, B.; Gutierrez-Puebla, E.; Iglesias, M.; Monge, M. A.; Ruiz-Valero, C.; Snejko, N. *Inorg. Chem.* **2002**, *41*, 2429.

10.1021/cm049527r CCC: $27.50
Published on Web 06/18/2004

vanadium, chromium, and aluminum dicarboxylates.[21−26] Concerning iron, the high trend of iron(III) to produce oxides when starting under hydrothermal conditions seems to have ruled out the existence of such Fe^{3+}-based solids. In contrast, iron(II) compounds were numerous.[16,17,27−34]

We recently developed a controlled secondary building unit (SBU) approach using trimeric inorganic metal clusters (three metallic octahedra shared by μ_3-O), which keeps the integrity of the inorganic precursor during the formation of the solid. It involves acetates of trivalent transition metals (Fe, Cr, V, Ru, Mn, Co, etc.),[35,36] as precursors, which already present these trimers. It allowed the rational synthesis of two new open framework iron(III) dicarboxylates built up from trimers of iron octahedra and dicarboxylates.[37] According that the iron trimers could decompose under hydro- or solvothermal conditions, it was assumed that some new coordination frameworks built up from a mixture of trimers and single octahedra could be isolated. We present here a new three-dimensional iron(III) dicarboxylate, obtained starting from trimeric iron(III) acetate, that exhibits both trimers and monomers. The crystallographic characterization from X-ray powder data, some magnetic data, and a thermal study involving X-ray thermodiffractometry and Mossbaüer experiments of the new three-dimensional iron(III) dicarboxylate, **MIL-85** or $Fe^{III}_2O\{O_2C-CH_3\}_2\{O_2C-C_6H_4-CO_2\}\cdot 2CH_3OH$, are reported.

Experimental Section

Synthesis. MIL-85 was solvothermally synthesized (autogenous pressure) from a mixture of iron(III) acetate $\{Fe^{III}(H_2O)\}_3O(O_2C_2H_3)_6\cdot 3H_2O\cdot Cl$, synthesized according to Dziobkowski et al.,[38] terephthalic acid $HO_2C-(C_6H_4)-CO_2H$ (Alfa 97%), sodium hydroxide (Aldrich, 99%), methanol (Prolabo, 99%), and H_2O in the molar ratio 1:3.0:1.5:1000:50. Iron acetate and terephthalic acid were first dispersed into methanol and stirred at room temperature; then, an aqueous solution of sodium hydroxide was added dropwise to the first solution. The resulting slurry was introduced into a Teflon-lined steel autoclave, and the temperature was set at 363 K for 5 days. The final pH remained slightly acidic (<4) during the course of the synthesis. A light orange powder was finally obtained together with traces of terephthalic acid. All the attempts for getting single crystals of **MIL-85** failed.

Density Measurement. The density measurement performed on **MIL-85**, using a Micromeretics apparatus Accupyc 1330, was 2.15(1) $g\cdot cm^{-3}$ (calcd: 2.37 $g\cdot cm^{-3}$).

Elementary Analysis. Quantitative elemental analyses indicated Fe and C contents respectively equal to 20.5 and 35.7%, whereas the theoretical values are 23.6 and 35.4%, respectively. The default in iron is probably due to the presence of residual terephthalic acid which decreases the iron content and increases the carbon percentage. The X-ray refined quantitative content of terephthalic acid has been estimated at 7%; considering its density (1.5 $g\cdot cm^3$) and composition, it gives a theoretical density for **MIL-85** in the presence of residual terephthalic acid of 2.30 $g\cdot cm^3$ and Fe and C contents of 22.0 and 36.9%.

Thermogravimetry. TGA experiments, performed under air atmosphere (2 °C/min) on **MIL-85** using a TA-Instrument type 2050 analyzer apparatus have shown two weight losses of 13.5% and 54% at approximately 373 and 573 K corresponding, respectively, to the departures of the free methanol and of one bound methanol group, followed by the loss of organic moieties. At higher temperatures, the residue is iron oxide (see Thermal Behavior section). These losses are in agreement with the theoretical values (13.5 and 52.7%).

Infrared Spectroscopy. The infrared spectra of the title compounds clearly show the presence of the vibrational bands characteristic of the framework −(O−C−O)− groups around 1550 and 1430 cm^{-1} confirming the presence of the dicarboxylate within the solid. Bands around 3500 cm^{-1} also confirmed the presence of −OH groups.

Temperature-Dependent X-ray Diffraction. X-ray thermodiffractometry, performed in the furnace of a Siemens D-5000 diffractometer in the $\theta-\theta$ mode under air, shows several steps in the decomposition for **MIL-85** (see Thermal Behavior section) and the reversible dehydration of **MIL-85**. Each pattern was recorded within the range 7−30° (2θ) with 2s/step scan which gave an approximate 1 h length for each pattern at the corresponding temperature. The heating rate between two temperatures was 5 °C/min.

Mössbauer Spectrometry. First experiments were carried out by means of a bath cryostat, using a constant acceleration spectrometer and a Co source diffused into a Rh matrix. The evolution of the sample was followed versus temperature using a cryofurnace, with successive annealing under vacuum for 1 h and in situ cooling at 77 K for collecting a Mössbauer spectrum. The values of the isomer shifts are quoted relative to an α−Fe foil at 300 K. The hyperfine parameters were refined using a least-squares fitting procedure in the MOSFIT program.[39]

Magnetic Measurements. Experiments were performed on a powder sample of **MIL-85** over the temperature range of 5−300 K, with a SQUID magnetometer for an external applied magnetic field B of 0.1 T. The samples were first zero field cooled and the magnetic field was applied after stabilization of the temperature at 4.5 K.

Sorption Experiments. The surface area was measured on **MIL-85** outgassed overnight at 100 °C with a Micromeretics ASAP 2010 apparatus using nitrogen (N_2) as the adsorbed gas.

Results and Discussion

Structure Solution. All attempts for getting single crystals of **MIL-85** failed. Consequently, X-ray diffraction patterns of **MIL-85** were collected on a powdered sample using a D5000 ($\theta-2\theta$ mode) Siemens diffractometer with λ(Cu $K\alpha_1$, $K\alpha_2$) = 1.5406, 1.5444 Å.

(21) Barthelet, K.; Adil, K.; Millange, F.; Serre, C.; Riou, D.; Férey, G. *J. Mater. Chem.* **2003**.
(22) Barthelet, K.; Marrot, J.; Riou, D.; Férey, G. *Angew. Chem., Int. Ed* **2002**, *41*, 281.
(23) Barthelet, K.; Riou, D.; Férey, G. *Chem. Commun.* **2002**, 1492.
(24) Millange, F.; Serre, C.; Férey, G. *Chem. Commun.* **2002**, 822.
(25) Serre, C.; Millange, F.; Thouvenot, C.; Nogues, M.; Marsolier, G.; Louër, D.; Férey, G. *J. Am. Chem. Soc.* **2002**, *124*, 13519.
(26) Loiseau, T.; Serre, C.; Huguenard, C.; Fink, G.; Taulelle, F.; Henry, M.; Bataille, T.; Férey, G. *Chem.−Eur. J.* **2004**, *10*, 1.
(27) Riou-Cavellec, M.; Albinet, C.; Livage, C.; Guillou, N.; Nogues, A.; Grenèche, J. M.; Férey, G. *Solid State Sci.* **2002**, *4*, 267−270.
(28) Riou-Cavellec, M.; Férey, G. *Solid State Sci.* **2002**, *4*, 1221−1225.
(29) Sanselme, M.; Riou-Cavellec, M.; Férey, G. *Solid State Sci.* **2002**, *4*, 1419−1424.
(30) Kim, Y. J.; Jung, D. Y. *Bull. Korean Chem. Soc.* **1999**, *20*, 827−830.
(31) Kim, Y.; Jung, D. Y. *Bull. Korean Chem. Soc.* **2000**, *21*, 656−658.
(32) Kim, Y. J.; Jung, D. Y. *High-Pressure Res.* **2001**, *20*, 99−107.
(33) Kumagai, H.; Chapman, K. W.; Kepert, C. J.; Kurmoo, M. *Polyhedron* **2003**, *22*, 1921−1927.
(34) Zeng, M. H.; Gao, S.; Yu, X. L.; Chen, X. M. *New J. Chem.* **2003**, *27*, 1599−1602.
(35) Cannon, R. D.; White, R. P.; Lippard, Ed.: London, 1987; Vol. 36.
(36) Hataway, B. J.; Wilkinson, G., Ed.; Pergamon: Oxford, 1987; Vol. 2, pp 439−441.
(37) Serre, C.; Millange, F.; Surblé, S.; Férey, G. *Angew. Chem., Int. Ed* **2004**, accepted for publication.
(38) Dziobkowski, C. T.; Wrobleski, T. J.; Brown, D. B. *Inorg. Chem.* **1982**, *20*, 671.
(39) Teillet, J.; Varret, F. MOSFIT program, unpublished.

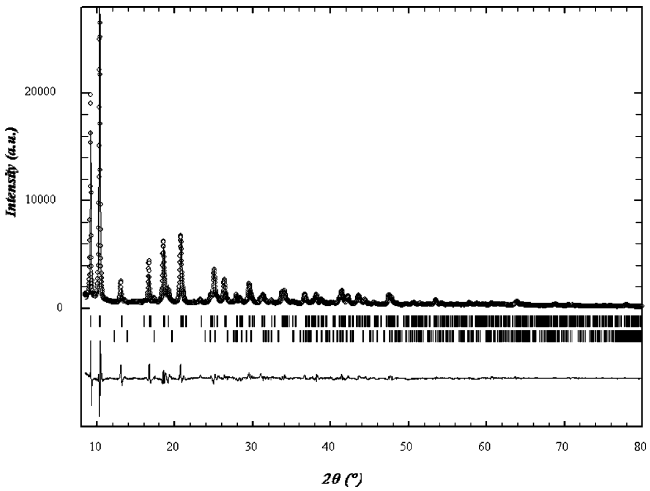

Figure 1. Final Rietveld plot of **MIL-85**.

Table 1. Atomic Coordinates for MIL-85

atom	*x/a*	*y/b*	*z/c*
Fe(1)	0.642(1)	−0.195(1)	0.078(1)
Fe(2)	0.812(1)	−0.053(1)	0.255(1)
O(1)	0.807(2)	−0.048(2)	0.143(1)
O(2)	0.210(4)	−0.166(3)	0.559(4)
O(3)	0.492(3)	−0.223(4)	0.160(1)
O(4)	0.024(4)	−0.170(4)	0.689(2)
O(5)	0.018(4)	0.081(2)	0.273(3)
O(6)	0.678(2)	−0.358(3)	0.091(1)
O(7)	0.307(3)	0.260(4)	0.488(1)
O(8)	0.742(4)	−0.703(4)	−0.133(2)
O(9)	0.584(3)	−0.068(2)	0.081(2)
O(10)	0.699(2)	0.048(3)	0.257(1)
O(11)	0.096(1)	−0.276(3)	0.791(2)
C(1)	0.244(4)	−0.256(4)	0.553(1)
C(2)	−0.025(8)	−0.182(2)	0.745(2)
C(3)	−0.141(5)	−0.331(5)	0.752(1)
C(4)	−0.134(3)	−0.433(2)	0.715(1)
C(5)	−0.262(3)	−0.549(7)	0.692(1)
C(6)	0.400(2)	−0.220(3)	0.570(1)
C(7)	0.474(7)	−0.177(2)	0.636(2)
C(8)	−0.233(6)	−0.386(10)	0.810(2)
C(9)	0.715(2)	−0.346(5)	0.024(2)
C(10)	0.852(2)	−0.599(3)	−0.108(1)
C(11)	0.455(6)	0.003(6)	−0.245(1)
C(12)	0.876(11)	−0.272(7)	0.025(2)
C(13)	0.847(3)	−0.491(8)	−0.061(1)
C(14)	−0.269(4)	−0.423 (6)	0.555(4)

The X-ray diffraction pattern of **MIL-85** has been successfully indexed using the Dicvol software,[40] leading to the hexagonal space groups $P6_1$ (no. 169) or $P6_5$ (no. 170) with $a = 11.045$ (1) Å, $c = 18.823$ (1) Å. The pattern matching was performed with Fullprof2k using the WinPLOTR software package.[41,42] Its structure was solved in the space group $P6_1$ using Expo.[43] The iron atoms and most of the oxygen atoms were found upon the direct method , whereas the remaining oxygen and carbon atoms were located during Fourier difference maps using the SHELXTL software.[44] Soft distances and angles constraints have been applied during the refinement both for the iron octahedra and the organic linkers. The final structure was then refined using Fullprof2k. Terephthalic acid was found as a small impurity and refined as a secondary phase. Bond valence calculation[45] leads to the values of 2.9(1) and 2.9(1) for the valence of iron atoms for **MIL-85** which is in agreement with the presence of trivalent iron.

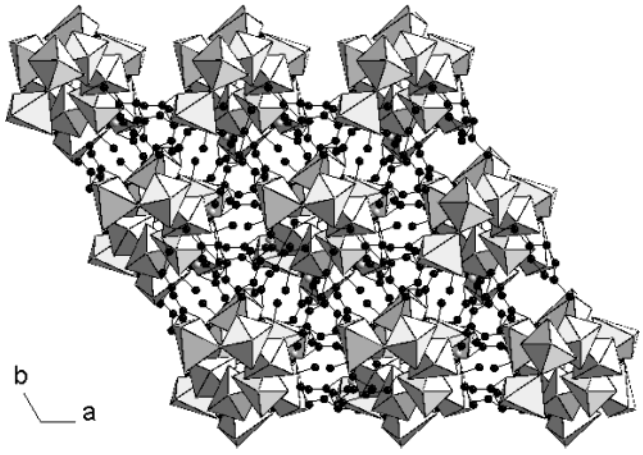

Figure 2. View of the structure of **MIL-85** along the *c* axis. Iron octahedra and carbon atoms are represented in light gray and black, respectively.

Table 2. Principal Bond Lengths (Å) for MIL-85

Fe(1)−O(1)	2.12(3)	Fe(1)−O(3)	2.17(4)
Fe(1)−O(6)	2.04(4)	Fe(1)−O(7)	2.02(3)
Fe(1)−O(8)	2.10(3)	Fe(1)−O(9)	1.82(3)
Fe(2)−O(1)	2.10(3)	Fe(2)−O(1)	2.12(2)
Fe(2)−O(2)	2.00(4)	Fe(2)−O(4)	1.92(3)
Fe(2)−O(5)	2.03(5)	Fe(2)−O(10)	2.04(5)
O(2)−C(1)	1.24(4)	O(3)−C(1)	1.16(4)
O(4)−C(2)	1.17(3)	O(5)−C(2)	1.20(5)
O(6)−C(9)	1.30(4)	O(7)−C(9)	1.30(3)
O(8)−C(10)	1.27(4)	O(9)−C(10)	1.36(3)
O(10)− C(11)	1.51(5)	O(11)−C(14)	1.42(4)
C(1)−C(6)	1.59(6)	C(2)−C(3)	1.50(5)
C(3)−C(4)	1.35(4)	C(3)−C(8)	1.41(3)
C(4)−C(5)	1.42(8)	C(5)−C(6)	1.40(6)
C(6)−C(7)	1.44(8)	C(7)−C(8)	1.44(6)
C(9)−C(12)	1.53(5)	C(10)−C(13)	1.51(5)

The formula deduced from the structure determination for **MIL-85** is $Fe^{III}_2O\{O_2C-CH_3\}_2\{O_2C-C_6H_4-CO_2\}\cdot 2CH_3OH$. The final agreement factors[46] (see Supporting Information) are rather satisfactory: $R_p/R_{wp} = 10.6$ and 13.9%, $R_{Bragg}/R_F = 8.1$ and 7.0%. The final Rietveld plot is reported in Figure 1. Atomic coordinates and bond distances are given in Tables 1 and 2.

Discussion. MIL-85 exhibits a three-dimensional structure built up from iron(III) octahedra linked to terephthalate dianions and acetate groups creating a three-dimensional framework with a 1-d small-pore channel system (Figure 2). Free methanol molecules are present within the pores interacting both through hydrogen bonds with terminal methanol molecules and acetate groups via van der Waals interactions.

Iron octahedra are linked through corner-sharing μ_3-O atoms (O(1)) to form a one-dimensional helical inorganic chain (Figure 3). These inorganic chains can be described in two different ways: (1) a central corner-sharing chain of iron octahedra ($Fe(2)O_6$) with a second

(40) Boultif, A.; Louër, D. *J. Appl. Crystallogr.* **1991**, *24*, 987.
(41) Rodriguez-Carvajal, J. In *Collected Abstracts of Powder Diffraction Meeting, Toulouse, France*; 1990; p 127.
(42) Roisnel, T.; Rodriguez-Carvajal, J. In *Abstracts of the 7th European Powder Diffraction Conference, Barcelona, Spain*; 2000, p 71.
(43) Altomare, A.; Burla, M. C.; Camalli, M.; Carrozzini, B.; Cascarano, G. L.; Giacovazzo, C.; Guagliardi, A.; Moliterni, A. G. G.; Polidori, G.; Rizzi, R. *J. Appl. Crystallogr.* **1999**, *32*, 339.
(44) *SHELXL97*, University of Göttingen, Germany, 1997.
(45) Brese, N. E.; O'Keeffe, M. *Acta Crystallogr.* **1991**, *B47*, 192.
(46) Young, R. A.; Wiles, D. B. *J. Appl. Crystallogr.* **1982**, *15*, 430.

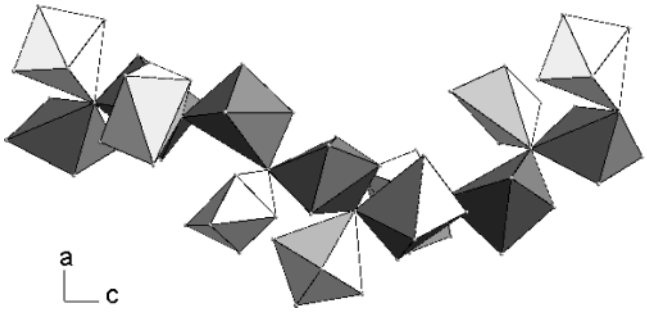

Figure 3. View of the inorganic chains of **MIL-85**. For a better understanding, iron octahedra $Fe(1)O_6$ and $Fe(2)O_6$ are represented in white and gray, respectively.

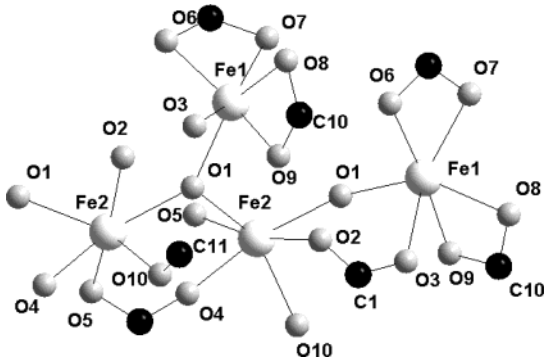

Figure 4. View of the structural unit of **MIL-85**. Oxygen and carbon atoms are represented in light gray and black, respectively.

iron octahedra ($Fe(1)O_6$), grafted to the chain through the μ_3-O atom (O(1)), turning around through the 6_1 screw axis; (2) a connection of trimers, built up from one $Fe(1)O_6$ octahedron and two $Fe(2)O_6$ octahedra, and one single $Fe(1)O_6$ octahedron. Thus, the inorganic subnetwork of **MIL-85** can be considered as a reminiscence of the initial trimeric iron acetate. These latter consist of three iron octahedra which share one μ_3-O oxygen atom; six acetate groups connecting the iron atoms bridging two different consecutive iron octahedra; one terminal water molecule completes the coordination sphere of each iron atom. The trimer is probably partially destroyed under solvothermal conditions into single iron complexes, and the formation of the chains of **MIL-85** would come from the linkage of residual trimers and isolated iron complexes.

Two different environments are present for iron atoms in the structure (Figure 4). Fe(1) is surrounded by four oxygen atoms from two chelating acetate groups (O(6), O(7) and O(8), O(9)), one μ_3-O oxygen atom (O(1)) and one oxygen atom from the terephthalate (O(3)); the presence of two acetate groups directly bonded to the metal creates a strongly distorted environment for Fe(1). The second iron octahedron ($Fe(2)O_6$) exhibits a more regular environment with three oxygen atoms from the terephthalate (O(2), O(4), O(5)), one μ_3-O oxygen atom (O(1)) and one terminal methanol moiety (O(10)). Bond valence calculations give a valence of 1.25 for the μ_3-O atom (O(1)) which is lower than expected. This comes from the use of laboratory powder data and the low parameter/independent reflection ratio (<3) which allows us to propose an approached structure for **MIL-85**. A valence of 2.9 is also calculated for both Fe(1) and Fe(2) which is in agreement with further Mössbauer and magnetic results.

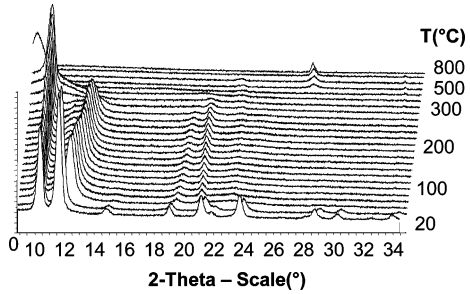

Figure 5. X-ray thermodiffractogram of **MIL-85** under air; for a better understanding, a 2θ offset is applied for each pattern. The TGA of **MIL-85** is represented as an insert at the top of the figure.

The interatomic distances are on the whole close to those usually reported for iron(III) solids: Fe−O distances are between 1.82 and 2.17 Å, while C−O and C−C distances are usual for both the carboxylates (1.17−1.36 and 1.35−1.59 Å, respectively) and methanol groups (1.42 and 1.51 Å).

The channels are delimited by the benzene rings of the terephthalate, oxygen atoms of the iron polyhedra, and terminal $-CH_3$ groups from the acetate moieties. Thus, free methanol molecules, located within the pores, are interacting both with oxygen atoms of the inorganic chains and carbon atoms of the organic moieties. The CH_3 groups of the acetate molecules are either pointing at the benzene rings within the core of the helical chains (C(9)) or at the pore channels (C(13)) interacting with the methanol groups.

The departure of the terminal methanol molecules does not destabilize the framework (see Thermal Behavior section) and we assume that the high-temperature form of **MIL-85** contains both five- and six-coordinated iron metal sites (see Mössbauer Results). Besides, it is noteworthy that the synthesis of **MIL-85** can be achieved over a large range of temperature: at room temperature, the synthesis time increases up to several months (>3) and X-ray diffraction confirms that **MIL-85** is formed; at 100 °C, one night is necessary; whereas the use of higher temperatures (>110 °C) leads to dense phases.

Thermal Behavior. A first X-ray thermodiffractometry experiment was performed under air atmosphere between room temperature and 800 °C (1173 K) for **MIL-85**. As shown in Figure 5, **MIL-85** is on the whole stable up to 275 °C. The departure of methanol groups, which occurs between 50 and 200 °C, leads to a significant pore contraction. This latter can be estimated following the evolution of the *hkl* reflections of **MIL-85**: it can be seen that the *a* parameter is almost stable, increasing slightly from 11.04 to 11.20 Å, while the *c* parameter decreases strongly from 18.8 to 12.6 Å; it gives at 200 °C an approximate cell volume of 1370 $Å^3$, indicating a pore contraction of ∼30%. Despite the contraction, **MIL-85** retains a small porosity as shown by a nitrogen adsorption experiment which leads to a Langmuir surface area of 110 m^2/g with a type I isotherm characteristic of microporous solids. At higher temperatures, the departure of the organic moieties leads to the destruction of the framework and to the crystallization of iron oxide Fe_2O_3.

In a second step, the study of the reversibility of the solvent departure in **MIL-85** was performed using X-ray

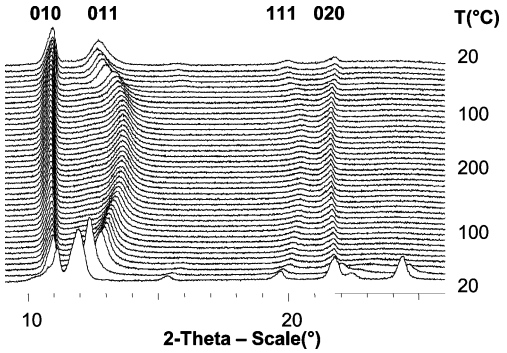

Figure 6. Study of the dehydration−hydration process of **MIL-85** using an X-ray thermodiffractogram of **MIL-85** under air; for a better understanding, a 2θ offset is applied for each pattern.

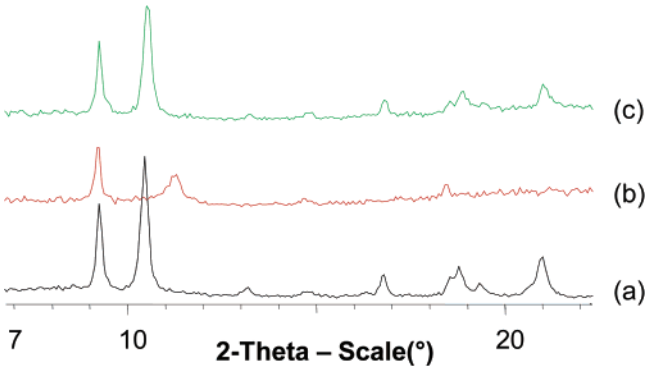

Figure 7. X-ray diffraction pattern of **MIL-85**: (a) as-synthesized; (b) heated at 200 °C and cooled to room temperature; (c) heated at 200 °C, cooled to room temperature, wetted with water, and finally dried at room temperature.

thermodiffractometry by heating and cooling between room temperature and 200 °C (473 K) (Figure 6). It appears clearly that this process is reversible, i.e., the methanol molecules being replaced by water molecules during the cooling process, indicating a zeolithic behavior for **MIL-85**. The crystallinity of **MIL-85** observed when back to room temperature is, however, worse than that of the initial product; this is probably due to the hydrophobic character of the pore walls which leads to a slow replacement of the methanol groups by water molecules; however, the initial crystallinity of **MIL-85** is fully recovered by wetting **MIL-85** using water (Figure 7).

Mössbauer Spectrometry. ^{57}Fe Mössbauer spectra of **MIL-85**, performed at both 300 and 77 K, are paramagnetic doublets. In Figure 8, one observes the 77 K paramagnetic doublet which exhibits broadened and asymmetrical lines: the hyperfine structure is well described by means of at least two quadrupolar components without applying any constraints. Experimental proportions (48 and 52% for Fe(1) and Fe(2) at both 300 and 77 K) are in agreement with those expected(50, 50%) on the basis of the crystallographic results. The isomer shift values are characteristic of high-spin-state iron(III), while the values of the quadrupolar splitting are quite different for the two sites: 0.46 and 0.78 mm·s^{-1}. It is difficult to attribute a priori, in a first step, the two iron sites at this stage.

Some Mössbauer spectra recorded at 77 K corresponding to annealing treatments for 1 h are presented in Figure 9. A progressive broadening of the low energy

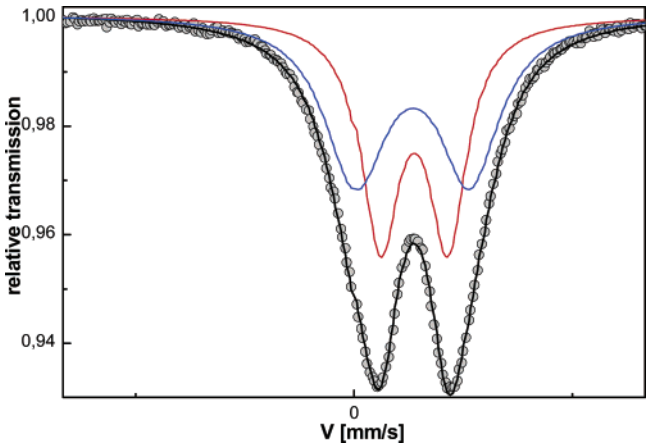

Figure 8. Mössbauer results operated at 77 K on **MIL-85** as-synthesized.

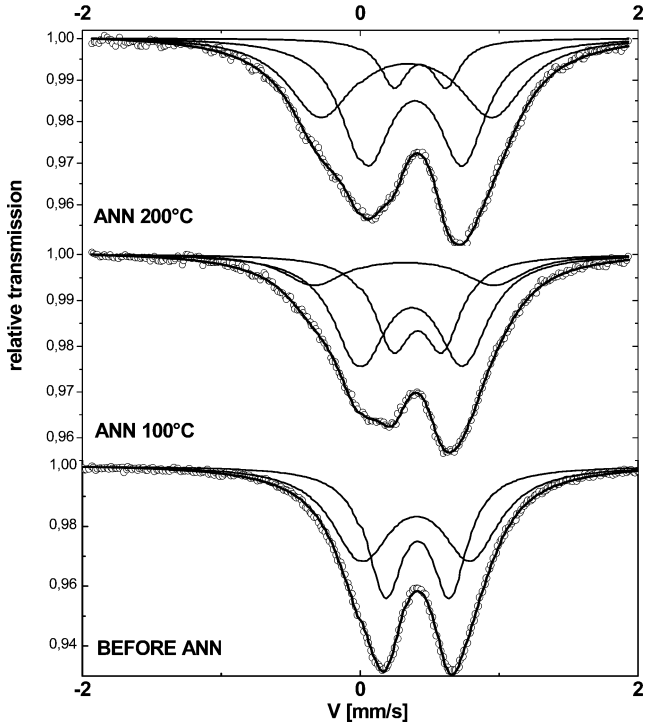

Figure 9. Mössbauer results operated at 77 K on **MIL-85** before annealing, and after annealing at 100 and 200 °C under vaccum.

quadrupolar line can be observed. The analysis of the hyperfine structure using three quadrupolar doublets reveals the occurrence of an additive quadrupolar component with a lower isomer shift value. This is due to the lowering coordination from octahedral to pentahedral environment that is consistent with results established from X-ray diffractometry. The plot of the relative proportion of each quadrupolar component versus the annealing temperature clearly confirms this phenomenom (Figure 10). Indeed, it is in agreement with the loss of one terminal methanol group for Fe(2) upon heating, leading to a pentahedral high-spin-state iron(III). One can thus attribute the low and the high quadrupolar splitting component to the iron, Fe(2) and Fe(1), respectively. Indeed, this is consistent with a strongly distorted environment for the Fe(1) octahedron due to the two acetate groups chelating directly bound

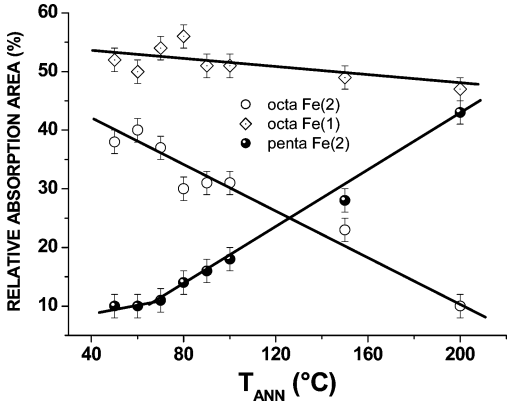

Figure 10. Evolution of the relative proportion of the quadrupolar components of **MIL-85** as a function of the annealing temperature treatment between 25 and 200 °C.

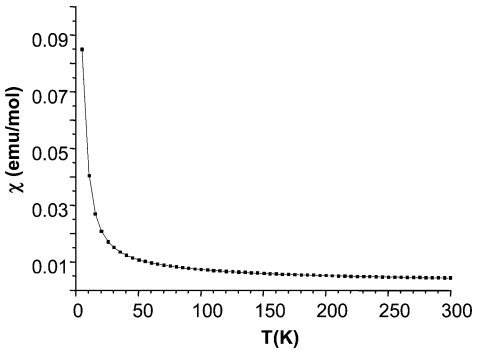

Figure 11. Susceptibility measurement versus temperature of **MIL-85**.

to the iron atom introducing O−O distances of 2.2 Å instead of 2.8 Å in a regular octahedron.

Magnetic Properties. The inverse molar susceptibility curve $1/\chi_{dc}$ reveals a paramagnetic behavior in the whole temperature range (Figure 11). The fit of the linear part of $1/\chi_{dc}$, established after correction of the sample holder signal and the core diamagnetism, follows a Curie−Weiss law $\theta_{dc} = C/(T - \theta_p)$. This leads to a negative paramagnetic Curie temperature (of approximately $\theta_p = -300$ K), indicative of antiferromagnetic interactions at very low temperatures ($T_N < 5$ K). It is important to emphasize that the extremely large value of $|-\theta_p/T_N|$ suggests the presence of highly frustrated antiferromagnetic interactions in agreement with the 120° angle of Fe^{3+} polyhedra in the cluster. For Fe^{3+}, the orbital momentum is quenched so that S is the appropriate quantum number: $\mu_{eff} = g[S(S + 1)]^{1/2}\,\mu_B$, with $g = 2$ and $S = {}^5/_2$ (high spin). This leads to $\mu_{eff} = 5.9(2)\,\mu_B$, value deduced from magnetic measurements performed on three different samples. The Curie constant deduced from the linear part of the $1/\chi_{dc}$ curves gives an effective moment $\mu_{eff} = 4.74\,\mu_B$ per iron atom or $\mu_B = 8.48\,\mu_B$ per formula unit for **MIL-85**.

Conclusion

Finally, **MIL-85** is a new example of three-dimensional iron(III) dicarboxylate obtained from trimeric acetate precursors. Its exhibits interesting properties such as a chiral one-dimensional inorganic sub-network, the presence of unsaturated metal sites upon heating, a high thermal stability, and a zeolithic behavior. However, unlike the case of the two previously reported iron dicarboxylates, which kept intact the initial trimeric secondary building units (SBUs), the partial destruction of the trimers leads in this case to a three-dimensional solid with a one-dimensional inorganic subnetwork. This shed some light on the various structural possibilities issued from this trimeric SBU route which can lead to structures with a wide range of inorganic subnetworks starting from trimers up to chains of octahedra and all the possible intermediate combinations of building units resulting from the degradation under solvo- or hydrothermal conditions of the initial trimeric precursors. Other research is in progress using trimeric metal acetates and will be published soon.

Supporting Information Available: Crystal data and structure refinement parameters for **MIL-85** (pdf). This material is available free of charge via the Internet at http://pubs.acs.org.

CM049527R